

Correlated hopping in the Falicov-Kimball model: A large-dimensions study

Avraham Schiller

Racah Institute of Physics, The Hebrew University, Jerusalem 91904, Israel

(May 10, 2018)

The Falicov-Kimball model with a correlated-hopping interaction is solved using an extended dynamical mean-field theory that becomes exact in the limit of large dimensions. The effect of correlated hopping is to introduce nonlocal self-energy components that retain full dynamics as $D \rightarrow \infty$, thus introducing an explicit k -dependence to the single-particle self-energy. An explicit solution for the homogeneous phase at $D = 2$ reveals significant nonlocal dynamical contributions in the physically relevant regime of a moderately large correlated-hopping amplitude, indicating that important nonlocal correlations are omitted in Hubbard-like models upon neglecting the correlated-hopping interaction.

PACS numbers: 71.10.Fd, 71.27.+a, 71.30.+h

The development of the limit of infinite dimensions,¹ or the Dynamical Mean-Field Theory (DMFT), has opened exciting new possibilities in the study of correlated electron systems.² One notable example is the Mott-Hubbard metal-insulator transition realized in $V_{2-y}O_3$ and $Ca_{1-x}Sr_xVO_3$, where the main features of the optical conductivity and the photoemission data are successfully accounted for within the DMFT treatment of the single-band Hubbard model.^{3,4} This approach, however, fails to explain the moderate mass enhancement and the apparent k -dependence of the single-particle self-energy close to the transition in these materials,^{5,6} indicating that important nonlocal interactions are either omitted in the Hubbard model, or mistreated in the DMFT.

One nonlocal interaction term clearly absent in the Hubbard model is that of correlated hopping (CH), in which hopping between neighboring lattice sites depends on the occupancy of the opposite spin orientation. Such an interaction term is an integral part of the Coulomb repulsion between electrons, and with estimates ranging from about 0.5eV in transition metals,⁷ to 0.8eV in the cuprates,⁸ and up to 3.3eV in benzene,⁹ it is certainly comparable to, if not larger than, the corresponding amplitude for single-particle hopping in real systems. Despite this fact and in spite of Hirsch's suggestion of a new mechanism for superconductivity,¹⁰ there is still no qualitative understanding of the effects that a CH term might have. While some rigorous statements can be made, these are restricted to certain models in one spatial dimension,^{11–14} and to a few very special cases in higher dimensions.^{14–16} There is thus an obvious need for a careful investigation of CH within a reliable non-perturbative approach, applicable to the entire range of interactions from weak to strong coupling.

In this paper, we generalize the limit of infinite dimensions, $D \rightarrow \infty$, as to include the CH interaction. Focusing on the Falicov-Kimball model¹⁷ — a simplified Hubbard model with one spin species tied down — the effect of CH is to introduce *nonlocal* self-energy components that retain full dynamics as $D \rightarrow \infty$. This marks departure from the local approximation. Similar

to existing formulations of the infinite-dimensional limit, though, both the local and nonlocal self-energy components are extracted from an effective single-site action, which can still be treated analytically for the Falicov-Kimball model. Solving the resulting DMFT for the homogeneous phase at $D = 2$ and in the physically relevant regime of a moderately large CH amplitude, the dynamical contribution of the nearest-neighbor self-energy is found to be comparable to that of the local self-energy, indicating that important nonlocal correlations are omitted in Hubbard-like models upon neglecting the CH interaction. This not only suggests that CH may be essential for the complete understanding of the metal-insulator transition in $V_{2-y}O_3$ and $Ca_{1-x}Sr_xVO_3$, but further calls into question its omission in any Hubbard-like modeling of real systems.

We begin our discussion with the Hamiltonian

$$\begin{aligned} \mathcal{H} = & \frac{t_1}{\sqrt{2D}} \sum_{\langle i,j \rangle} \left\{ d_i^\dagger d_j + d_j^\dagger d_i \right\} + U \sum_i d_i^\dagger d_i f_i^\dagger f_i \\ & + \frac{t_2}{\sqrt{2D}} \sum_{\langle i,j \rangle} \left\{ d_i^\dagger d_j + d_j^\dagger d_i \right\} \left(f_i^\dagger f_i + f_j^\dagger f_j \right) \\ & + (E_f - \mu) \sum_i f_i^\dagger f_i - \mu \sum_i d_i^\dagger d_i, \end{aligned} \quad (1)$$

in which itinerant d fermions interact via an on-site Coulomb repulsion U with localized f fermions on a D -dimensional hypercubic lattice. Motion of the d fermions has two components: a single-particle, nearest-neighbor hopping term t_1 , and a correlated-hopping term t_2 , in which the hopping amplitude for the d fermions depends on the occupancy of the corresponding f fermions. The two fermion species share a joint chemical potential, μ .

For $t_2 = 0$, Eq. (1) reduces to the Falicov-Kimball model,¹⁷ which is perhaps the simplest many-body Hamiltonian to exhibit both a Mott-Hubbard metal-insulator transition and long-range ordered phases. A nonzero t_2 modifies the single-particle dynamics of the itinerant fermions in two ways. First, there is a straightforward Hartree renormalization of the static single-particle hopping amplitude according to $t_1 \rightarrow t = t_1 +$

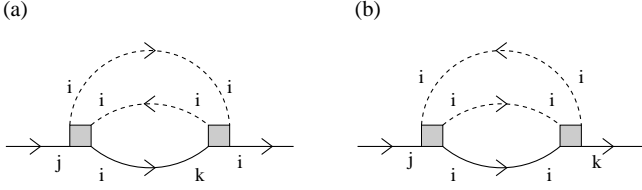


FIG. 1. Representative d self-energy diagrams. Here, squares indicate a correlated-hopping vertex (t_2); full (dashed) lines represent bare d (f) propagators; and j and k are distinct nearest neighbors of site i . In Fig. (a), there is summation over all equivalent sites k . The diagram of Fig. (a) gives a contribution of order $D^{-1/2}$ to Σ_{ij} , while the diagram of Fig. (b) gives a contribution of order D^{-1} to Σ_{kj} . Both terms are relevant in the limit $D \rightarrow \infty$.

$2n_f t_2$, where n_f is the f occupation number (assuming a homogeneous phase). In addition, the d and f fermions acquire new self-energy terms with full dynamics, which survive also in the absence of an on-site U . To investigate the effect of CH we employ the limit of large dimensions,¹ which has proven useful in studying the Falicov-Kimball model.^{18,19} To this end, both the single-particle and CH terms in Eq. (1) have been properly rescaled with D .

For conventional Hubbard-like models, the self-energy is purely local at $D = \infty$, rendering the local approximation exact. This paradigm breaks down as soon as CH is considered, as exemplified in Fig. 1 for the Hamiltonian of Eq. (1). In Fig. 1, sites j and k are distinct nearest neighbors of site i . Thus, after summation over all equivalent k , the diagram of Fig. 1(a) gives a contribution of order $1/\sqrt{D}$ to the nearest-neighbor d self-energy $\Sigma_{ij}(z)$, while the diagram of Fig. 1(b) (in which both j and k are fixed) gives a contribution of order $1/D$ to the next-nearest-neighbor self-energy $\Sigma_{kj}(z)$. Since both orders in D coincide with the necessary large- D rescaling of the corresponding nearest- and next-nearest-neighbor hopping amplitudes,²⁰ both self-energies contribute in the limit $D \rightarrow \infty$. As shown below, the nearest-neighbor and next-nearest-neighbor self-energies are in fact the only nonlocal self-energy components relevant at $D = \infty$.

A systematic formulation of the $D \rightarrow \infty$ limit for the Hamiltonian of Eq. (1) employs the Luttinger-Ward functional Φ — the sum of all vacuum-to-vacuum skeleton diagrams. Consider a generic Φ diagram. Labeling each vertex according to the site index of its incoming and outgoing f lines, we attach the $1/\sqrt{D}$ factor associated with each CH vertex to its incoming or outgoing nearest-neighbor d line. With this convention we notice that, even after summation over all intermediate sites, any path connecting two vertices at sites $i \neq j$ gives a contribution of order $D^{-\|i-j\|/2}$ or higher to the diagram at hand ($\|i-j\|$ is the minimal number of nearest-neighbor steps leading from site i to site j). Given that (i) any two vertices within a Φ diagram can be connected by four independent paths having no lines in common, and (ii) the total number of equivalent sites j scales as $D^{\|i-j\|}$, the overall contribution of such a diagram (after summation

over all equivalent j 's) is $\mathcal{O}(D^{-\|i-j\|})$. Thus, to order D^{-n} , only skeleton diagrams with a maximal inter-vertex distance $\|i-j\|_{max} \leq n$ need to be considered. Specifically, only purely local vertices are left at $D = \infty$.

While the above classification appears identical to that for conventional Hubbard-like models, it should be emphasized that purely local vertices in our convention do not imply purely local diagrams. To the contrary, a CH vertex at site i couples the operators d_i and f_i to the nearest-neighbor shell operator

$$\psi_i \equiv \frac{1}{\sqrt{2D}} \sum_{\langle j, i \rangle} d_j, \quad (2)$$

in which j is summed over the $2D$ nearest neighbors of site i . Thus, a CH vertex at site i necessarily introduces at least one propagator that is not confined to site i .

Despite the above nonlocality, the $D \rightarrow \infty$ limit remains tractable since Φ decouples in this limit into

$$\Phi = \sum_i \Phi_{loc}[G_{ii}^{dd}, G_{ii}^{d\psi}, G_{ii}^{\psi d}, G_{ii}^{\psi\psi}, G_{ii}^{ff}], \quad (3)$$

where Φ_{loc} is the functional generated by the action

$$\begin{aligned} S_{eff} = & - \int_0^\beta d\tau \int_0^\beta d\tau' \sum_{\alpha, \beta = d, \psi} \alpha^\dagger(\tau) [\mathcal{G}^{-1}(\tau - \tau')]_{\alpha\beta} \beta(\tau') \\ & - \int_0^\beta d\tau \int_0^\beta d\tau' f^\dagger(\tau) \mathcal{G}_f^{-1}(\tau - \tau') f(\tau') \\ & + t_2 \int_0^\beta d\tau \{d^\dagger(\tau) \psi(\tau) + \psi^\dagger(\tau) d(\tau)\} f^\dagger(\tau) f(\tau) \\ & + U \int_0^\beta d\tau d^\dagger(\tau) d(\tau) f^\dagger(\tau) f(\tau). \end{aligned} \quad (4)$$

Here $\mathcal{G}(\tau - \tau')$ is a 2×2 matrix propagator, chosen such that, when dressed with the effective-action self-energy, it coincides with the corresponding lattice propagator:

$$\mathcal{G}^{-1}(i\omega_n) = G^{-1}(i\omega_n) + \Sigma^S(i\omega_n) \quad (5)$$

with

$$G(i\omega_n) = \begin{bmatrix} G_{ii}^{dd}(i\omega_n), & G_{ii}^{d\psi}(i\omega_n) \\ G_{ii}^{\psi d}(i\omega_n), & G_{ii}^{\psi\psi}(i\omega_n) \end{bmatrix} \quad (6)$$

[$\omega_n = \pi(2n+1)T$ are the Matsubara frequencies]. Here, in using the 2×2 matrix notation of Eqs. (5)–(6), we have identified the indices $\alpha = d, \psi$ with $\alpha = 1, 2$, respectively. Contrary to \mathcal{G} , which requires knowledge of the fully dressed lattice d propagator, the bare f propagator in Eq. (4) is simply $\mathcal{G}_f^{-1}(i\omega_n) = i\omega_n + \mu - E_f$, which stems from the localized nature of the f fermions.

From Eq. (3) it is apparent that Φ at $D = \infty$ is a functional of the local d and f propagators, as well as the nearest-neighbor and next-nearest-neighbor d Green functions which enter via $G_{ii}^{d\psi}, G_{ii}^{\psi d}$, and $G_{ii}^{\psi\psi}$. Thus, in

addition to the local d and f self-energies, one must also consider the nearest- and next-nearest-neighbor d self-energies. From a functional derivative of Eq. (3) one has

$$\Sigma_{ii}(i\omega_n) = \Sigma_{dd}^S(i\omega_n) + \Sigma_{\psi\psi}^S(i\omega_n), \quad (7a)$$

$$\Sigma_{<ij>}(i\omega_n) = \frac{1}{\sqrt{2D}} [\Sigma_{d\psi}^S(i\omega_n) + \Sigma_{\psi d}^S(i\omega_n)], \quad (7b)$$

$$\Sigma_{\ll ij \gg}(i\omega_n) = \frac{1}{2D} N_{\ll ij \gg} \Sigma_{\psi\psi}^S(i\omega_n), \quad (7c)$$

where $\ll ij \gg$ denotes distinct lattice sites with a common nearest neighbor. In Eq. (7c), $N_{\ll ij \gg}$ is equal to one for i and j on the same axis; otherwise it is equal to two. Accordingly, the \vec{k} -dependent d self-energy reads

$$\Sigma_{\vec{k}}(z) = \Sigma_{dd}^S(z) + \epsilon_{\vec{k}} [\Sigma_{d\psi}^S(z) + \Sigma_{\psi d}^S(z)] + \epsilon_{\vec{k}}^2 \Sigma_{\psi\psi}^S(z), \quad (8)$$

where $\epsilon_{\vec{k}} = \sqrt{2/D} \sum_{l=1}^D \cos(k_l)$. Notice that, contrary to conventional formulations of the limit of large dimensions, $\Sigma_{\vec{k}}$ has an explicit \vec{k} dependence which enters solely through the dimensionless energy $\epsilon_{\vec{k}}$: $\Sigma_{\vec{k}}(z) \equiv \Sigma_{\epsilon_{\vec{k}}}(z)$.

A self-consistency loop can finally be closed by expressing the lattice Green function of Eq. (6) in terms of $\Sigma_{\vec{k}}$. For the spatially homogeneous phase this gives

$$G(z) = \int_{-\infty}^{\infty} d\epsilon \frac{\rho(\epsilon)}{z + \mu - t_1 \epsilon - \Sigma_{\epsilon}(z)} \begin{bmatrix} 1, & \epsilon \\ \epsilon, & \epsilon^2 \end{bmatrix}, \quad (9)$$

where $\rho(\epsilon)$ is the density of states for the energy $\epsilon_{\vec{k}}$, i.e., a Gaussian for $D = \infty$. Equation (9) can further be written in closed form in terms of the bare ($U, t_2 = 0$) tight-binding d propagator. We also note that Eqs. (8)–(9) were derived under the explicit assumption of a hypercubic lattice with only nearest-neighbor single-particle hopping. Different self-consistency equations will generally apply to other lattices and other tight-binding models.

Equations (4)–(9) are an exact formulation of the limit $D \rightarrow \infty$ for the Hamiltonian of Eq. (1). In particular, for $t_2 = 0$, when only $\Sigma_{dd}^S(i\omega_n)$ is nonzero, they properly reduce to the corresponding equations for the Falicov-Kimball model at $D = \infty$.¹⁸ In the spirit of the DMFT, the same set of equations can also be applied to any finite dimension D , provided the actual D -dimensional density of states $\rho(\epsilon)$ is used in Eq. (9). Below we present results for $D = 2$. Although designed at present to describe the homogeneous phase, this formulation is easily extended to phases with long-range order, as well as to other lattice models with CH. For example, in the Hubbard model one has to introduce separate $\psi_{i\sigma}$ fields for each spin orientation, but the basic formulation remains the same.

A crucial advantage of the Hamiltonian of Eq. (1) over its Hubbard counterpart is that the action of Eq. (4) can be treated analytically. Integrating out the f particles, the lattice Green function of Eq. (6) is expressed as

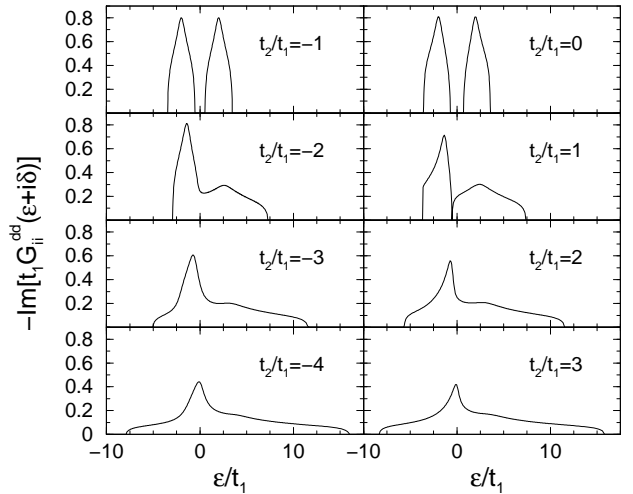


FIG. 2. The d spectral function as a function of t_2/t_1 , for $n_f + n_d = 1$, $U/t_1 = 4$, $T/t_1 = 1$, and $D = 2$. For both $t_2/t_1 = 0$ and $t_2/t_1 = -1$, the half-filled model is particle-hole symmetric, with a Mott gap for $U/t_1 = 4$. This gap gradually closes upon increasing $t_2/t_1 > 0$ or decreasing $t_2/t_1 < -1$, until the lower and upper Hubbard bands are merged into one broad band. Note the general resemblance between curves with values of t_2/t_1 that are symmetric about $t_2/t_1 = -1/2$.

$$G(i\omega_n) = (1 - n_f) \mathcal{G}(i\omega_n) + n_f \left[\mathcal{G}^{-1}(i\omega_n) - \begin{pmatrix} U & t_2 \\ t_2 & 0 \end{pmatrix} \right]^{-1}, \quad (10)$$

where n_f is the f occupation number: $n_f = 1/(e^{\beta\epsilon} + 1)$,

$$\epsilon = E_f - \mu + U/2 - \frac{1}{\beta} \sum_{n=-\infty}^{\infty} \ln \det \left[1 - \mathcal{G}(i\omega_n) \begin{pmatrix} U & t_2 \\ t_2 & 0 \end{pmatrix} \right]. \quad (11)$$

Once Eqs. (5), (9)–(11) have been iterated and the f occupation number determined, the same equations can be used to calculate $G(z)$ for an arbitrary complex z .

Restricting attention to $D = 2$ and $E_f = 0$, we focus hereafter on the homogeneous phase of the half-filled case: $n_f + n_d = 1$, where n_d is the d occupation number. Setting $U/t_1 = 4$ and $T/t_1 = 1$, Fig. 2 shows the evolution of the d spectral function as a function of t_2/t_1 . For the Falicov-Kimball model, $t_2 = 0$, the d spectrum has a Mott gap. This gap persists throughout the range $-1.4 \lesssim t_2/t_1 \lesssim 1$, although the chemical potential does not always fall inside the gap. For either $t_2/t_1 \gtrsim 1$ or $t_2/t_1 \lesssim -1.4$, the lower and upper Hubbard bands merge into one broad band, reflecting the increase in kinetic energy of the itinerant fermions. Due to the lack of particle-hole symmetry, the d spectrum is generally asymmetric. Indeed, only for $t_2 = 0$ and $t_2/t_1 = -1$ is the half-filled model particle-hole symmetric, in which case the resulting spectrum is temperature independent.²¹

As shown in Fig. 3, one cannot simply absorb t_2 into an effective Hartree renormalization of the single-particle hopping within the simpler Falicov-Kimball

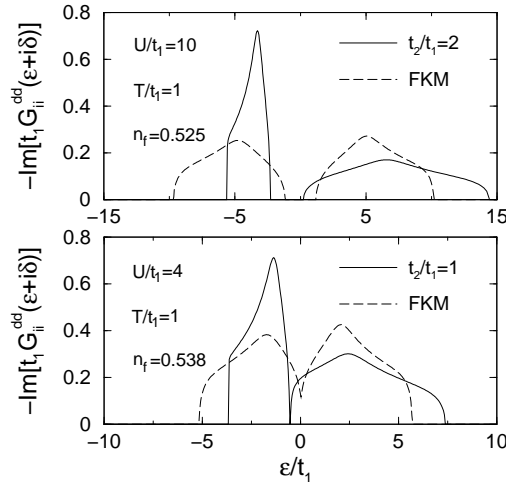


FIG. 3. The d spectrum for the Hamiltonian of Eq. (1) at $D = 2$ versus the one obtained within the DMFT for the Falicov-Kimball model with the renormalized single-particle hopping, $t_{FKM} = t_1 + 2t_2n_f$. Here n_f and $n_d = 1 - n_f$ are kept the same in both models, as are U/t_1 and T/t_1 .

model. Specifically, tuning μ and E_f in the latter model as to maintain the same n_f and n_d , there are substantial deviations between the d spectral function for the Hamiltonian of Eq. (1) and that obtained within the DMFT for the Falicov-Kimball model with the renormalized hopping, $t_{FKM} = t_1 + 2t_2n_f$. The d spectrum for a nonzero t_2 is notably more asymmetric, with considerable broadening (narrowing) of the upper (lower) Hubbard band.

The effect of CH is best seen, though, in the nonlocal d self-energy components, which are absent in the DMFT for $t_2 = 0$. Figure 4 depicts the imaginary parts of Σ_0 , Σ_1 , and Σ_2 , defined from the expansion $\Sigma_{\vec{k}} = \Sigma_0 + \Sigma_1\epsilon_{\vec{k}} + \Sigma_2\epsilon_{\vec{k}}^2$. From Eqs. (7)–(8), $\Sigma_1 = \sqrt{2D}\Sigma_{<i,j>}$ and $\Sigma_2 = 2D\Sigma_{<<i,j>>}/N_{<<i,j>>}$ are the appropriately scaled nearest-neighbor and next-nearest-neighbor self-energy components. Evidently, the imaginary part of Σ_1 (which has no Hartree contribution) is comparable to that of Σ_0 in the physically relevant regime, $|t_2/t_1| \gtrsim 1$. Hence, important nonlocal dynamical contributions are omitted in the DMFT upon neglecting t_2 .

Anticipating a qualitatively similar result for the Hubbard model, CH thus provides a natural mechanism for a strong k -dependence in the single-particle self-energy, including for $D \rightarrow \infty$. This may prove important, e.g., for the understanding of the apparent k -dependence and the moderate mass enhancement close to the metal-insulator transition in $V_{2-y}O_3$ and $Ca_{1-x}Sr_xVO_3$.^{5,6} Study of the Hubbard model along these lines is currently underway.

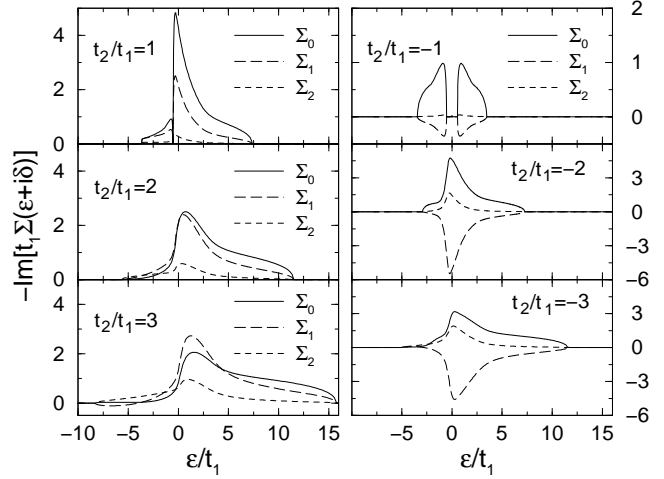


FIG. 4. Imaginary part of the d self-energy components Σ_0 , Σ_1 , and Σ_2 , defined from the expansion $\Sigma_{\vec{k}} = \Sigma_0 + \Sigma_1\epsilon_{\vec{k}} + \Sigma_2\epsilon_{\vec{k}}^2$ [see Eq. (8)], and related to the local, nearest-neighbor, and next-nearest-neighbor self-energies through $\Sigma_{ii} = \Sigma_0 + \Sigma_2$, $\Sigma_{<i,j>} = \Sigma_1/\sqrt{2D}$, and $\Sigma_{<<i,j>>} = N_{<<i,j>>} \Sigma_2/2D$ [see Eqs. (7)]. Here $n_f + n_d = 1$, $U/t_1 = 4$, $T/t_1 = 1$, and $D = 2$. In the physically relevant regime, $|t_2/t_1| \gtrsim 1$, the imaginary parts of Σ_1 and Σ_0 are comparable in size, indicating that important nonlocal dynamical contributions are omitted in the DMFT upon neglecting t_2 .

(1989).

² See, e.g., A. Georges *et al.*, Rev. Mod. Phys. **68**, 13 (1996).

³ M. J. Rozenberg *et al.*, Phys. Rev. Lett. **75**, 105 (1995).

⁴ M. J. Rozenberg *et al.*, Phys. Rev. Lett. **76**, 4781 (1996).

⁵ H.-D. Kim *et al.*, Phys. Rev. B **57**, 1316 (1998).

⁶ I. H. Inoue *et al.*, Phys. Rev. Lett. **74** 2539 (1995); I. H. Inoue *et al.*, Phys. Rev. B **58** 4372 (1998); H. Makino *et al.*, Phys. Rev. B **58** 4384 (1998).

⁷ J. Hubbard, Proc. Roy. Soc. London A **276**, 238 (1963).

⁸ J. Appel *et al.*, Phys. Rev. B **47**, 2812 (1993).

⁹ R. G. Parr *et al.*, J. Chem. Phys. **18**, 1561 (1950).

¹⁰ J. E. Hirsch, Phys. Lett. A **134**, 451 (1989); J. E. Hirsch and F. Marsiglio, Phys. Rev. B **39**, 11515 (1989).

¹¹ L. Arrachea and A. A. Aligia, Phys. Rev. Lett. **73**, 2240 (1994); L. Arrachea *et al.*, Phys. Rev. Lett. **76**, 4396 (1996).

¹² I. N. Karnaukhov, Phys. Rev. Lett. **73**, 1130 (1994); R. Bariev *et al.*, Europhys. Lett. **32**, 85 (1995).

¹³ A. Schadschneider, G. Su, and J. Zittartz, Z. Phys. B **102**, 393 (1997), and references therein.

¹⁴ J. de Boer *et al.*, Phys. Rev. Lett. **74**, 789 (1995); A. Schadschneider, Phys. Rev. B **51**, 10386 (1995).

¹⁵ R. Strack and D. Vollhardt, Phys. Rev. Lett. **70**, 2637 (1993).

¹⁶ A. A. Ovchinnikov, Mod. Phys. Lett. B **7**, 1397 (1993).

¹⁷ L. M. Falicov and J. C. Kimball, Phys. Rev. Lett. **22**, 997 (1969).

¹⁸ U. Brandt and C. Mielsch, Z. Phys. B **75**, 365 (1989); *ibid.* **79**, 295 (1990); *ibid.* **82**, 37 (1991); U. Brandt and M. P. Urbanek, *ibid.* **89**, 297 (1992).

¹⁹ J. K. Freericks, Phys. Rev. B **47**, 9263 (1993); *ibid.* **48**, 14797 (1993).

¹ W. Metzner and D. Vollhardt, Phys. Rev. Lett. **62**, 324

²⁰ E. Müller-Hartmann, Z. Phys. B **74**, 507 (1989).

²¹ This stems from the fact that T enters $G(z)$ in our formulation only through n_f and μ , which are fixed at $n_f = 1/2$ and $\mu = U/2$ for both $t_2 = 0$ and $t_2/t_1 = -1$.